Advances in Computational Sciences and Technology
ISSN 0973-6107 Volume 10, Number 5 (2017) pp. 1057-1080

http://www.ripublication.com

An Efficient Classification of MRI Brain Images and 3D Reconstruction Using Depth Map Estimation

M.Fathima Zahira[1] and M.Mohamed Sathik[2]

[1]Assistant Professor, Department of Computer Science, Syed hameedha Arts and Science College, Kilakarai,Tamilnadu, India.

[2]Principal, Sathakathullah Appa College, Thirunelveli, Tamilnadu, India.

Abstract

Digital Image processing is applied under the area of medicine so as to distinguish the ailments in the body of humans. The three dimensional reconstruction (3D) of tumor from the medicinal images is a significant procedure in the area of medicine while it assists the physicians in identification, surgical planning and biological investigation. This article includes two phases namely, i) Classification and ii) 3D reconstruction. Originally the input image is obtained from the MRI database which then undergoes skull stripping is a pre-processing phase for identifying the brain tumor that purges the redundant borough from the image. In the classification phase, the skull Stripped images undergoes segmentation by means of the watershed algorithm so as to identify the segmented tumor. Then from the segmented image the attributes such as shape, intensity and texture are extorted. Subsequently the attributes are lessened via the Principle Component Analysis (PCA). Depending upon the condensed attributes, the probabilistic neural network classifier categorizes the normal and the abnormal (tumor) images. The next phase is the 3D reconstruction phase, we intended the depth assessment for the skull stripped image by means of the guided filter. When the depth is attained, the visual relic of the created left view and right view images yields the ultimate 3D reconstruction outcomes.

Keywords: Skull stripping, Watershed segmentation, PNN classifier, Principle Component analysis (PCA), 3D Reconstruction, Magnetic Resonance Image (MRI), Depth-map estimation.

1. INTRODUCTION

MRI (Magnetic resonance imaging) is the frequently employed imaging modality for non-pertinent study of the brain tumor. This Magnetic resonance imaging utilizes radio waves and the magnetic fields so as to attain a collection of cross sectional images of brain [9]. In the past decade, the skull stripping has been considered as the main pre-processing phase in the applications of brain images and for subsequent psychiatry of MRI brain images [10]. The mechanical brain tissues segmentation from the MRI images is an exigent procedure owing to the deviation in the shapes of brain and resemblance of intensity value in the brain and the non-brain tissues. Skull stripping helps us to eliminate the non-brain tissue which is a vital phase in neuro-imaging research [11]. In accordance with the images of brain it imparts signals of brain anatomy it is helpful in the recognition of several brain glitches like malevolent glioma tumor and the skull have resembled intensity that make the automatic tumor detection tricky. In order to conquer this confront, the skull-stripping technique is preferred as a pre-processing phase for brain tumor recognition [5]. The Skull stripping techniques which exist in the literature are generally categorized into three types namely a) Region-based methods ii) edge-based methods and iii) hybrid methods [6][7]. The extortion of three dimensional objects and its visualization is the significant phase in the psychiatry of the pre-processed medicinal image statistics which facilitates to carry out diagnosis, treatment planning and treatment deliverance. Hence habitually, the radiation oncologists expend a significant part of their instance which performs the segmentation chore physically by employing one of the obtainable visualization and segmentation apparatus [1] [3].

The major chore of reconstruction is alienated into sub tasks. Initially preprocessing phase is carried out on the images in order to perk up the image quality. After that segmentation takes place so as to segment the tumor region [12]. Several segmentation approaches are employed in skull stripping analysis; the most frequent techniques are region growing, tumor detection via FPCM. Detection of tumor via symmetry psychiatry [17], watershed segmentation, threshold based segmentation, Otsu's approach [13], kapurs approach and histogram thresholding [14], in our approach watershed technique is employed for segmentation. The key plus of our approach is its simplicity and heftiness.

The classification phase includes two techniques. The first one is supervised learning technique where the Artificial Neural Network [19], Support Vector Machine [18] and the K-Nearest Neighbor [20] are employed and the other one is the unsupervised learning technique for clustering the data such as Self Organizing Map and K-means Clustering[15]. In our paper, the supervised learning technique which means the KNN is applied as it yields improved accuracy of categorization and performance.1) It is typically quicker to train a PNN network than the multilayer perceptron (MLP) network. 2) The PNN networks are frequently more precise than the MLP networks. 3) PNN networks are comparatively insensible to the outliers i.e., wild spots. 4) The PNN networks produce or engender precisely envisaged target possibility scores. 5) The PNN networks move towards to the Bayes optimal categorization [16].

Yet, owing to the deficiency of three dimensional medicinal fillings, transforming the conventional two dimensional contents into the three dimensional contents for emerging the three dimensional markets is incredibly essential and significant. The two dimensional to three dimensional conversion is separated into two techniques namely, i) semi-automatic and ii) full-automatic methods. Though the semi automatic adaptation approach [4] is extensively applied till nowadays, it needs substantial instant and human resources. Therefore, it is essential to build up full automatic conversion approaches for providing the three dimensional fillings simply. The fully automatic 2D to 3D conversion is then classified into two techniques: The first technique depends upon the depth map and the next technique depends upon the sparse 3D information of the attribute image spots. The approach applying the depth map is known as depth image based rendering i.e.,DIBR [5][6]. The extortion of depth is the vital in the course of conversion. The most dissimilarity amid the 2 dimension and the 3 dimension image is the depth information [7]. The depth cues based techniques allocates the depth values by means of image categorization, machine learning, depth from focus or the defocus, depth from the geometric view, depth from the texture gradient, depth from the comparative height and depth from the multi scale local and the inclusive image attributes [8].

2. RELATED WORK

A general complexity for the sole channel is that main current three dimensional reconstruction procedure depends upon the two dimensional motion are the nonlinear iterative forms. For further suitable exploit of real time relevance's, Youngmo Han *et.al* [21] have projected an systematic explanation form of 3D reconstruction method as an alternative of the nonlinear iterative forms. To obtain an analytical resolution, that paper introduced a notion which devises a human body joint as the two dimensional universal joint approach in place of the widespread three dimensional spherical joint replicas. In order to conquer the main constraint of the analytical solution type method, which means less precision, that article devises the estimation procedure as an optimization trouble. The procedure thus deliberated was employed to every joint in the human body continuously.

Na-Eun Yang *et.al* [22] projects an interacted technique of depth map creation from a sole image for the two dimensional to three dimensional conversion. With the help of the theory of depth distinction can lessens the human endeavor to engender a depth map. The main term essential from a user was to spot few prominent regions to be recognized based upon the depth variation. The intended technique builds theory of every prominent region and engenders a depth map of an input image.

Cheolkon Jun *et.al* [23] have intended a two dimension to three dimension conversion with motion-type adaptive depth assessment. Due the significant depth cue was motion parallax in that technique, initially the motion assessment was performed amid the chronological video frames. After that, a motion type adaptive technique was introduced to depth map assessment as the videos holds dissimilar depth arrangement based upon the motion type. Particularly, depth from the motion was used to

approximate the depth maps in place of global movement whereas the depth maps were engendered depending upon the depth from template with the local motion guided refinement in place of local motion. Ultimately, the DIBR technique was used to create the stereoscopic virtual scenes from the depth maps.

Weicheng Huanga *et.al* [24] have introduced a fresh 2 dimension to 3 dimension video conversion approach enthused by the psychophysical facts of the person visual processing of three dimensional views and by the topical replicas of innate three dimensional scene data. The main involvement was that they intended a global depth optimization procedure which entirely pools the two dimensional color and three dimensional innate view data through spatial depth coherence. The phrases depictive of these arithmetical and structural constrictions in the intended target role give out as burly and valuable priors on optimization. The Bayesian inference structure formulates it probable to oblige the three dimensional product regarding the arithmetical genuineness and structural reliability. The technique obtained from that replica yields premium depth propagation above the whole two dimensional video which paves the way for an enhanced value of experience while observing the two dimensional to three dimensional rehabilitated content.

Wei Liu*et.al* [25] have intended a proficient technique for the two dimensional to three dimensional video adaptation depending upon the structure from motion i.e., SFM. The main involvement holds a piecewise SFM technique and a new nonlinear depth warping representing the uniqueness of stereoscopic 3 dimensions. The dense depth maps were engendered and then treated by means of color segmentation.

3. PROPOSED WORK:

Our proposed work merely depends upon the medical image processing. We employs 3D reconstruction for proficiently analyze the MRI brain images. Brain tumor is the most hazardous ailment in humankind which is detected by the MRI scans that is the two dimensional image. Our intended scheme includes six phases namely, i) Preprocessing, ii) Segmentation, iii) Feature Extraction, iv) Feature selection, v) Classification, vi) 3D reconstruction.

Presume a database, $\{ IM_{mri} |$ MRI=1, 2... N$\}$ which includes the MRI brain images of $G(IM_{mri})$ both the normal and the abnormal (tumor) MRI brain images. In our approach, Originally the input image is obtained from the MRI database which then undergoes skull stripping is the preprocessing phase for identifying the brain tumor that purges the redundant zone from the image. The preprocessed image then undergoes segmentation via the Watershed technique so as to segment the tumour component individually. The attributes are extorted depending upon the shape, intensity and texture attributes. After that the attributes are abridged by means of Principle Component Analysis. Subsequently, classification is carried out by means of the PNN classifier. The 3D Reconstruction is performed by means of the ensuing images attained from the preprocessing stage.

Our intended classification and 3D reconstruction steps are mentioned as follows

(i) Preprocessing:
- Skull stripping

(ii) Segmentation
- Watershed algorithm

(iii) Feature Extraction
- Shape feature
- Intensity feature
- Texture feature

(iv) Feature Reduction
- Principle Component Analsis(PCA)

(v) Classification
- Probabilistic neural network (PNN) classifier

(vi) 3D Reconstruction

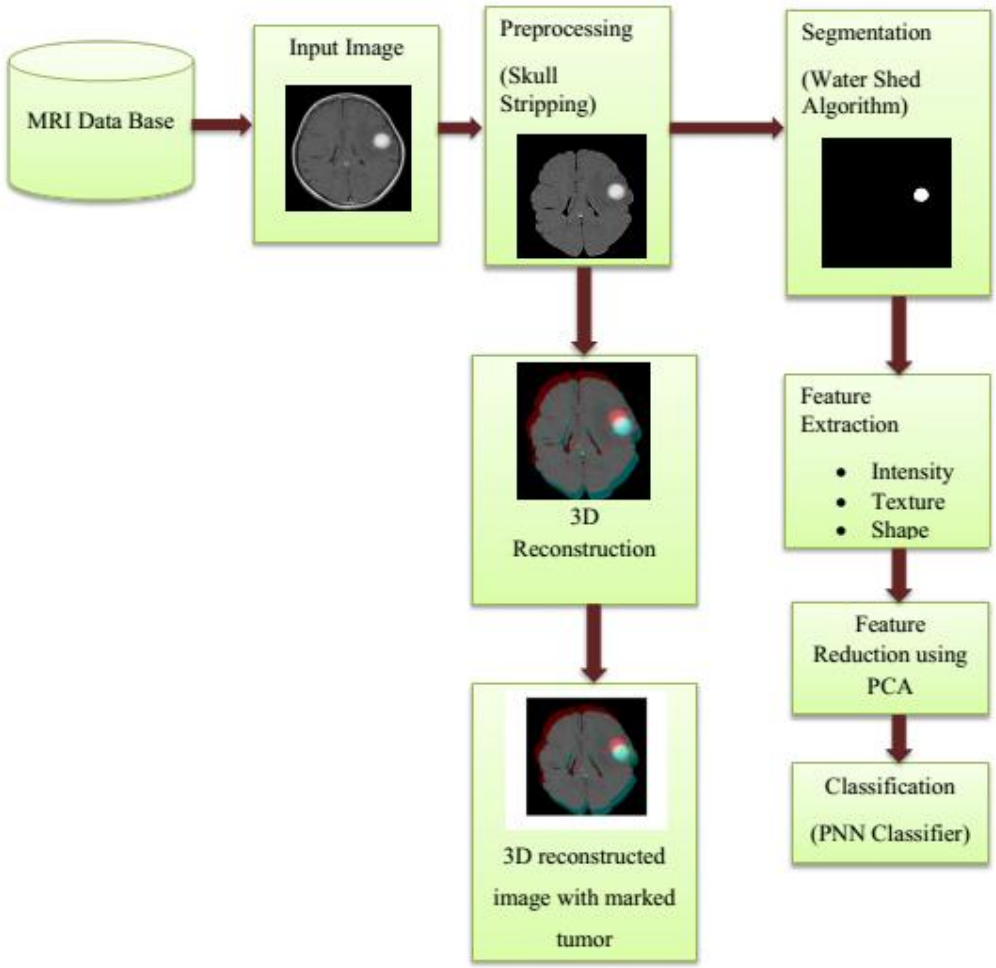

Fig 1: Architecture of our proposed 3D reconstruction method

3.1 PREPROCESSING

Preprocessing is a procedure to enhance the statistics of an image that represses the redundant distortions or for improving few attributes of an image essential for more processing.

3.1.1 Skull Stripping

The skull stripping method is employed to confiscate the skull from the MRI brain images. It splits the brain from the scalp, skull and the other adjacent portions of the brain. Originally the MRI brain image is fetched from the database which is then inputted for skull stripping. After that the subsequent process is pursued to purge the skull from the Brain images.

Step.1: Obtain the input image $G(IM_{mri})$ from the database db.

Step.2: Include variance to the input image $G(IM_{mri})$ by means of the subsequent equation.

$$G(IM_{mri}) = \sin(IM_{mri}{}^{3}/100)^{2} + \frac{1}{20} \times rand(size()\, IM_{mri}) \quad (1)$$

Step.3: Carry out the orthofit function on the input image (IM_{mri}) and the resultant image is epitomized as $T(IM_{mri})$.

Step.4: Find the max valued pixel (m) from the input image (IM_{mri}) and assess the limit (max (mx_c) & min (mn_c)) of the color range present on the image $T(IM_{mri})$.

Step.5: Approximate the normalized image by means of Eqn. (2)

$$g_r IM_{mri} = (TIM_{mri} - mx_C)/(mx_C - mn_C) \quad (2)$$

Step.6: Estimate the level of normalized image (τ) by applying the Otsu's approach for the orthofit image $T(IM_{mri})$.

Step.7: Compute the threshold for envisaging the filtered image ($fr(IM_{mri})$) using the subsequent eqn (3).

$$(fr(IM_{mri})) = g_r IM_{mri} \times (mx_C - mn_C) + mn_C \quad (3)$$

Step.8: Insert the pixels in to the filtered image $fr(IM_{mri})$ which surpass the threshold value calculated in step.6.

Step.9: Approximate the threshold (τ_1) by applying the Otsu's approach for the image assessed from the input image (IM_{mri}) by means of eqn (4).

$$\tau_1 = Otsu's\left(IM_{mri}/_{m}\right) \times m \tag{4}$$

Step.10: Insert the pixels in to the filtered image ($fr_1(IM_{mri})$) which surpass exceed the threshold value assessed in step.9.

Step.11: Surrogate the pixels of the filtered image ($fr(IM_{mri})$) obtained in step.6 by the filtered image obtained in $fr_1(IM_{mri})$.

Step.12: Carry out the opening process of the morphological function using the MATLAB function.

Step.13: Find the locale for diverse regions in the resulting image obtained in step.12, bounding box (pixels in the edges).

Step.14: Pick the region where the area exceeds 50000 pixels and its ensuing bounding box.

Step.15: Carry out the closing operation of morphological function on the image obtained in step.14 by means of the MATLAB function.

Step.16: Produce a mask with size of $w \times w_i$ and load the picked region inside its associated bounding box using the produced mask.

Step.17: Find the position of the one valued pixels and swap the one valued pixels by the original pixels in that location of the input image IM_{mri} .

The resultant image $Skt_r(IM_{mri})$ symbolizes the skull stripped image and it is used for further processing.

3.2 SEGMENTATION

3.2.1 Watershed Algorithm

The skull stripped image $Skt_r(IM_{mri})$ is given as input for segmentation for that we employs watershed segmentation approach for segmenting the tumor portion from the preprocessed image obtained from the prior phase.

Watershed segmentation is a gradient based segmentation approach. It contemplates the gradient map of an image as a relief map. By using this technique it segments the

image as a dam. The segmented parts are known as the catchment basins. This segmentation cracks several image segmentation troubles. It is appropriate for the images having high intensity value. This type of segmentation paves the way for over segmentation. In order to manage the over segmentation problem, the marker controlled watershed segmentation is employed. The sobel operator is appropriate for detecting the edges. In marker controlled watershed segmentation, sobel operator is employed to separate the object edge

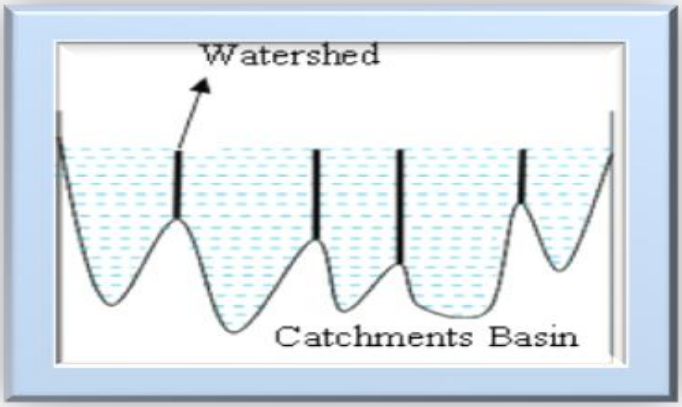

Fig 2: Watershed technique

This technique ideally symbolizes a gradient based segmentation technique where the different gradient values are considered as different heights. A hole is formed in every local minimum and soaks up in water and the water increases up to the local maxima. Once the two water bodies congregate each other, a dam is appropriately built amid them. The water climbs gradually as each and every point in the map are entirely soaked up. The image is successfully isolated by the dams. Now, the dams are called the watersheds and the separated regions are called the catchments basins.

By the way, the 'Topography' holds a measure to the source of watershed technique that gracefully outlines this technique tailor made for image segmentation. The water from the site draws off in the basin or the body of the river suitably named as the 'catchment basin'. The strength of water is considerably improved, if the water is exhausted in a frenziedly way to the catchment basin. The adjacent catchment basins are separated by the lines with more height or dams marked as the watershed lines with the purpose of distinguishing the water bodies in the dissimilar catchment basins. While the water is drain off in the target reservoir, it is hard to determine the precise catchment basin where it belongs. As it results in the classification of each point based upon if it belong to the catchment basins or else to the watershed. Until all maximum points are engrossed the draining of water is sustained. All the image pixels become an ingredient of the watershed or the catchment basin in this novel watershed approach which theoretically and practically carried out the image segmentation concern. As a result, all the image pixels develop the piece of the catchment basins is

detached in an indistinguishable label and the further pixels creates piece of the watershed are situated in different labels.

Steps to segment an image using watershed segmentation

- ✓ The gradient magnitude of the image is successfully assessed by means of the sobel edge mask. The image gradient is typically stumpy at the object core and soaring at the object bounds.
- ✓ Then, the dark regions of the image are marked as foreground objects. The foreground markers symbolize the linked blobs of pixels in all objects. The morphological approaches such as the 'opening by construction' and 'closing by construction' create regional maxima inside all objects.
- ✓ The Opening by reconstruction operation symbolizes an erosion function whose creation is escorted by means of the morphological renovation function. The closing operation gracefully maneuvers obvious of dark spots and the stem marks from the image. Yet, the equivalent opening by reconstruction and closing by reconstruction operations do not affect any interruptions to the object shapes. Subsequently, the regional maxima are assessed to attain outstanding foreground markers.

The aforementioned are the procedure needed for the widespread watershed approach for performing segmentation. The morphological functions such as the erosion and dilation operations are gracefully used for efficiently positioning the foreground.
The product attained signifies the segmented tumor *tmr* carried out by the novel watershed approach.

3.3 FEATURE EXTRACTION:

The segmented tumor achieved from the last step then undergoes feature extraction for extracting the different shape, intensity and texture features.

Shape features

1. Circularity
2. Area
3. Perimeter

Intensity features

1. Mean
2. Standard deviation
3. Variance

Texture features

1. Homogeneity
2. Contrast
3. Correlation
4. Energy

Therefore the ten attributes extracted in the feature extraction phase are inputted to the neural network classifier for categorization.

3.4 FEATURE REDUCTION via PCA

The chief notion of feature subset assortment is to eliminate the surplus or the inappropriate attributes from the data set which paves the way for reducing the classification accurateness and the redundant raise of calculation cost.

The feature reduction is carried out by means of the PCA technique. It is one of the dimensional reduction approaches of feature reduction technique so as to lessen the dimension of the dataset with no loss in data. PCA is employed on data prior to clustering will fallout more precise and lessens the time significantly. This approach is employed for visualization of data and noise diminution. This PCA technique is useful for compressing the data which exist in the more no of original variables into a novel array of small composite dimension and the data loss is less.

The steps for Principal Component Analysis technique is mentioned below:

1) Obtain the Eigen faces for the training images as $F = \{f_1, f_2, \cdots f_i\}; i = 1,2, \cdots N$ and then obtain the maximum Eigen value from the array of Eigen faces which is characterized as F^h. Subsequently calculate the covariance matrix for the every Eigen faces by means of eqn (5),

$$COV(Y) = \left(\frac{1}{N} \sum_{i=1}^{N} YY^T \right) \tag{5}$$

Where,

Y represents the matrix vectors characterized as $Y = \{\nu_1, \nu_2, \cdots \nu_k\}$

2) The matrix values are calculated by computing the dissimilarity amid each face from the average value of the every faces from F, which is mentioned in eqn (6),

$$\nu_k = \left(f_i - \left(\frac{1}{N} \sum_{i=1}^{N} f_i \right) \right) \tag{6}$$

3) The orthonormal vectors $ON = \{on_1, on_2, \cdots on_i\}$ forms the array of vectors G and compute the weight vector for the distinct Eigen faces f_i by means of following equation,

$$\varpi_i = \left(on_i^T \left(f_i - \left(\frac{1}{N} \sum_{i=i}^{N} fi \right) \right) \right) \tag{7}$$

4) Obtain the score value by calculating the Euclidean distance amid the weight vector and the image weight value as,

$$P = \left\| (w_i - \varpi_i) \right\|^2 \tag{8}$$

Where w_i signifies the weight value of the image i. The values attained as P is given to the subsequent phase for classification.

3.5 CLASSIFICATION

The outcome of feature reduction is employed for categorization by means of PNN classifier. PNN depends upon the hypothesis of the assessment of probability density function and the Bayesian classification approaches. The PNN classifier is separated into four layers depending upon its function. The four layers are mentioned below:

- ✓ Input layer
- ✓ Hidden layer
- ✓ Pattern layer or Summation layer
- ✓ Output layer

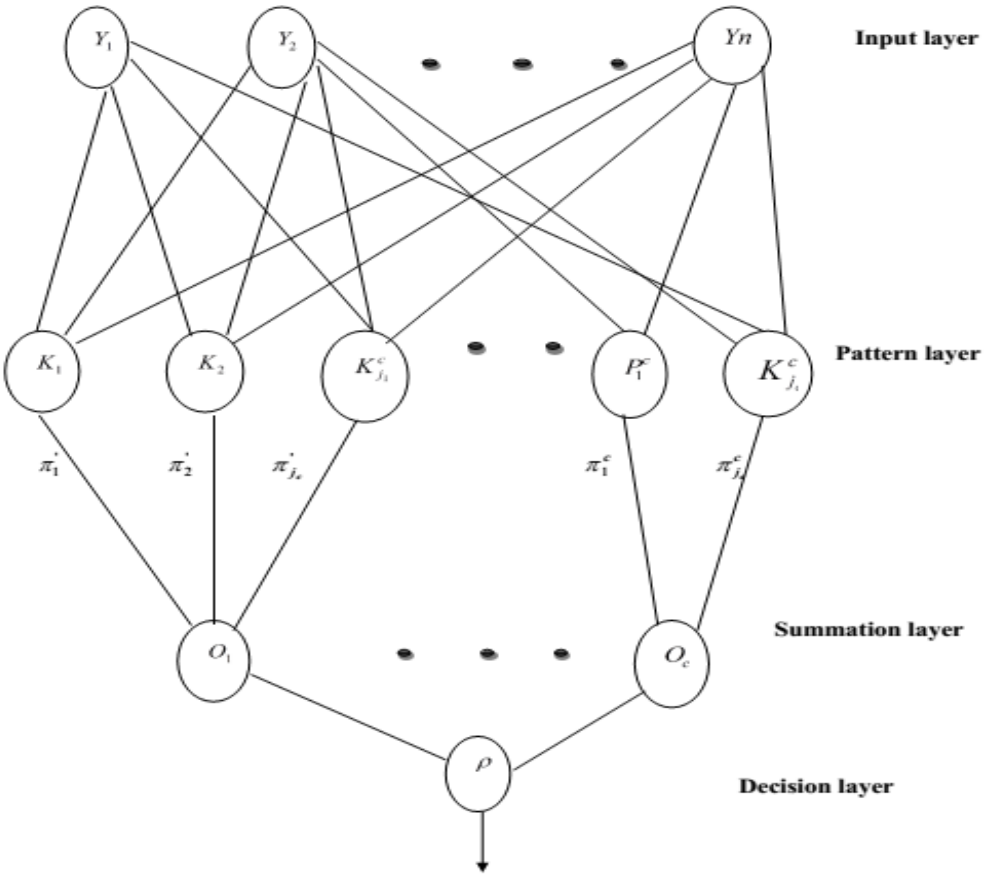

Fig 3: Probabilistic Neural Network classifier

The Probabilistic networks classifies based upon the Bayesian hypothesis, it is vital to categorize the input vectors into any one of the two classes by means of Bayesian optimal approach. This hypothesis offers a cost function to encompass the fact that it might be poorer to wrongly categorize a vector which is really a member of class A than it is to wrongly categorize a vector which belongs to class B. The Bayes rule categorizes an input vector that belongs to class A as:

Assume two classes A and B

- Originally the input vector is categorized by means of Baye's rule,

$$P_A K_A f_A(y) > P_B K_B f_B(y) \tag{9}$$

Where

P_A denotes the Priori possibility of categorizing vectors,

K_A be the cost of classifying vectors and

$f_A(y)$ be the probability density function of class A.

- The PNN classifier employs the subsequent formula for estimating the Probability Density Function,

$$f_A(y) = \frac{1}{(2\prod)^{n/2}\sigma^n m_n} \sum_{i=1}^{m} \exp\left[-2\frac{(y - y_A)^r (y - y_{Ai})}{\sigma^2} \right] \tag{10}$$

Where

n denotes the dimension of the input vectors and

σ be the smoothing vector.

Subsequent to the completion of training process, the anomalous level brain tumor cells are classified on the whole by means of the Neural Network.

4. 3D RECONSTRUCTION

The 2D to 3D depth generation technique commonly deal with two confronts. The first is the depth regularity within the similar object. The next one includes recovering a suitable depth association amid all objects. In order to tackle these confronts, we produce a depth map assessment by means of guided procedure for computing the skull stripped image $Skt_r(IM_{mri})$. The general structure of 3D reconstruction is illustrated in fig.4

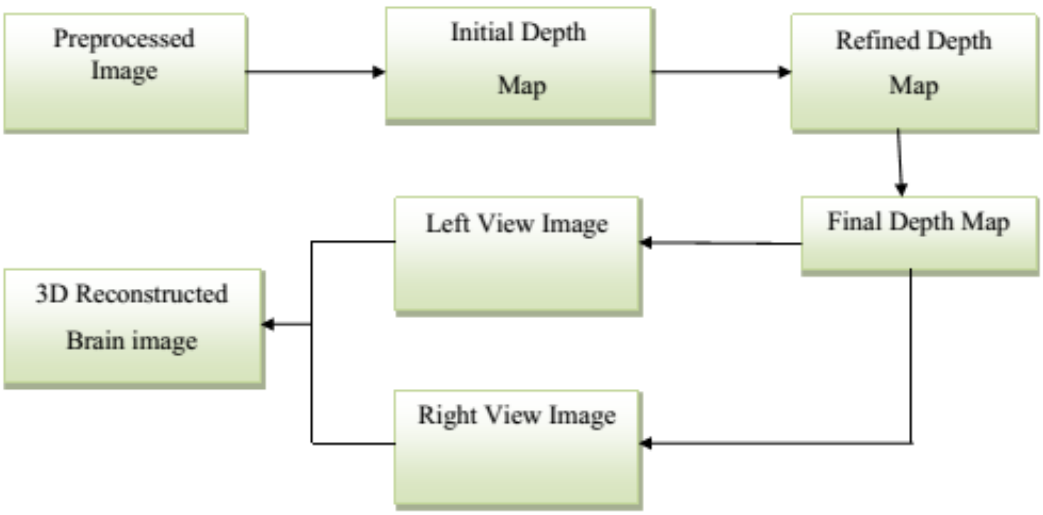

Fig 4: Architecture of 3D Reconstruction

4.1 Depth-map Estimation

The procedure of 3D reconstruction technique is described below:

The preprocessed image ($Skt_r(IM_{mri})$) is taken as input. Where (x, y) be the position coordinates of a pixel.

1) For the initial depth map, initially calculate the linear coefficients (d_k, e_k) for the guided filter:

$$d_k = \frac{1/|\omega| \sum IM_{mri}(x,y)\hat{m}(x,y) - u_k \overline{m_k}}{\sigma_k^2 + \in} \tag{11}$$

$$e_k = \overline{m_k} - d_k u_k \tag{12}$$

Where

$\hat{m}$ denotes the image of the guided filter,
$|\omega|$ be the number of pixels and
$\overline{m_k}$ be the mean of the image.

2) After calculating the linear (i_k, j_k), the filter $m'(x,y)$ is obtained by means of eqn (13)

$$m'(x, y) = d_k \hat{m}(x, y) + j_k \quad (13)$$

$\overline{m}$ denotes the initial depth map and the filter product m ' be the refined depth map.

3) The bilateral filter smoothens the images while maintaining the edges, thus exercised to eliminate the redundant information for the depth image m' anticipated by the technique offered above is efficiently detached [2].

4.2 3D Image Visualization using Depth Map-based Execution

When the depth map is attained, the parallax value is calculated for every pixel (x, y) in the predictable depth map. The parallax value is calculated by means of eqn (14)

$$\text{Parallax(x, y)} = \omega_3 * \left(1 - \frac{\hat{m}(x, y)}{ZPPL}\right) \quad (14)$$

Where ZPPL be Zero Parallel Plane and then deliberate the input image as the core view of the pair. Constant value ω_3 =0.5

To create the left view or the right view of the image, each pixel is moved by means of (x, y)/2 to the left or the right direction. Lastly the 3D reconstructed image is produced by pooling the parallax and the depth image.

5. RESULTS AND DISCUSSION

Our proposed image 3D Reconstruction technique is implemented in the MATLAB working platform of version 14a having the following machine configuration:

Processor: Intel core i3

OS: Windows 7

CPU speed: 3.20 GHz

RAM: 4GB.

In this part, the experimental outcomes for our intended approach are shown. The Skull stripping is an exigent and significant constituent of image processing and particularly for the MRI images. The freely obtained MRI image dataset was employed to estimate the intended watershed algorithm depending upon tumor segmentation and PNN classifier for categorizing the normal and the abnormal (tumor) images. We introduce a technique to examine the brain images and the 3D reconstruction of MRI images. Our intended approach is elaborately described in Section 3 and this part includes the elucidation on the accomplished outcome and the assessed performance.

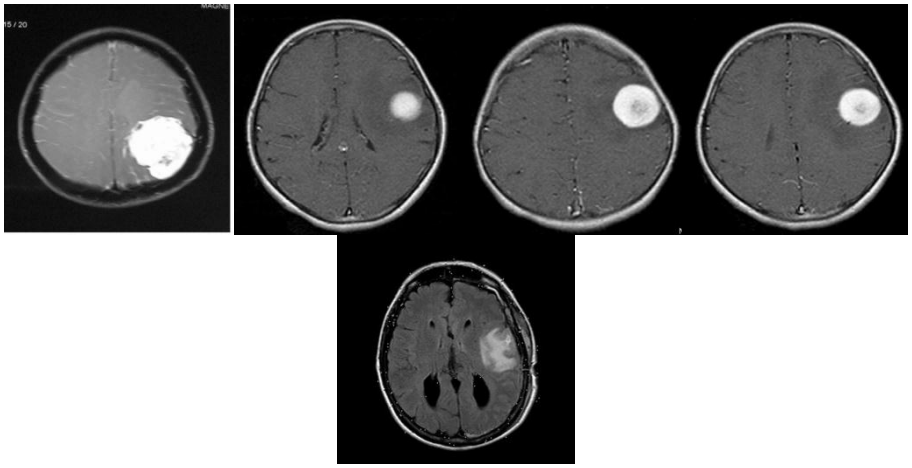

(a)

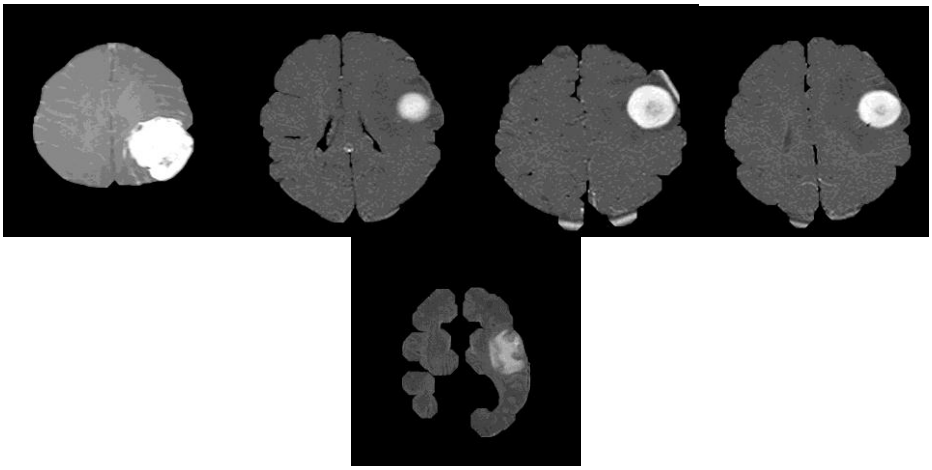

(b)

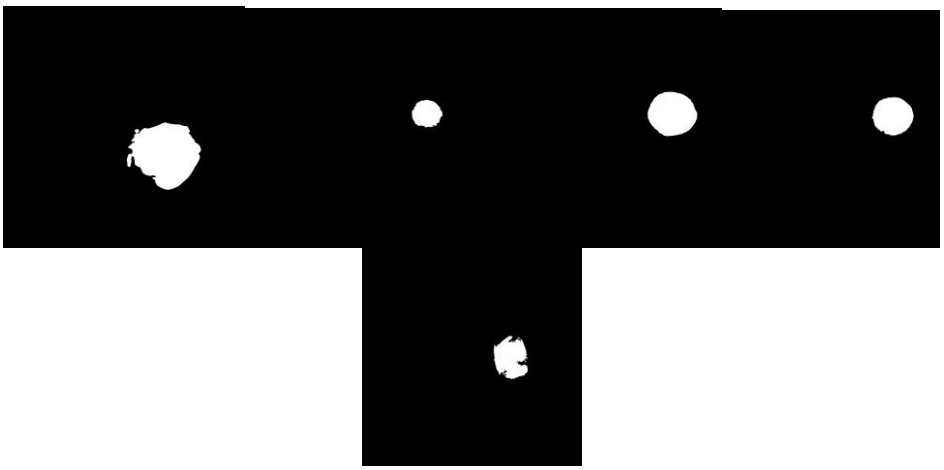

(c)

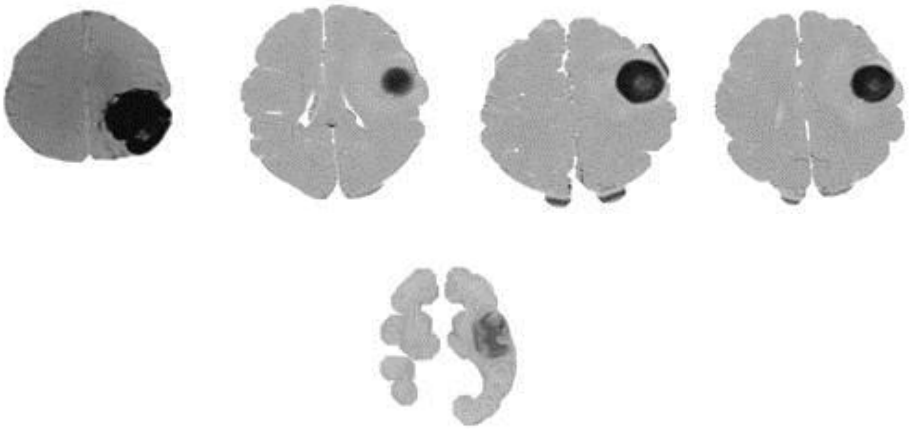

(d)

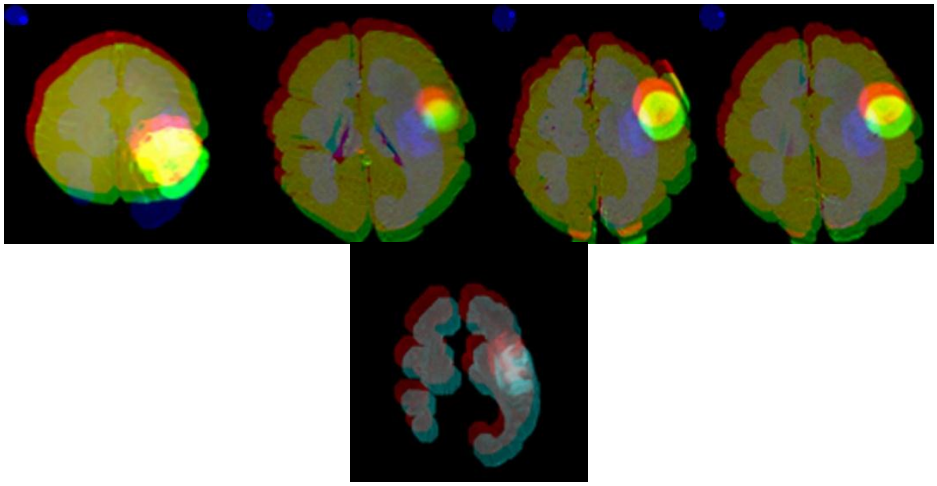

(e)

Fig 5: (a) Illustrates the sample images obtained from the database (b) skull stripped images (c) segmented image using watershed algorithm (d) Depth map estimation for 3D reconstruction (e) 3D reconstructed images

5.1 Performance analysis:

By means of the statistical metrics like sensitivity, specificity, accuracy, FNR and FPR, the performance of the intended tumor segmentation scheme is assessed. The statistical measurements of sensitivity, specificity, FPR, FNR and accuracy is articulated based on the TP, FP, FN and TN values.

Accuracy:
Accuracy is the percentage of the exact result; it may be true positive or true negative, in a population. It calculates the degree of realness of an analytical trial on a circumstance.

$$\text{Accuracy} = (\text{TN} + \text{TP})/(\text{TN} + \text{TP} + \text{FN} + \text{FP}) \tag{15}$$

Sensitivity:
It is the percentage of true positives which properly recognized by an analytical test. It exhibits how efficiently the test detects an ailment.

$$\text{Sensitivity} = \text{TP}/(\text{TP} + \text{FN}) \tag{16}$$

Specificity:
It is the percentage of the true negatives correctly recognized by an analytical test. It reveals how efficiently the test identifies the normal (i.e., negative) circumstance.

$$Specificity = \frac{TN}{FP + TN} \tag{17}$$

False Positive Rate (FPR):

The method of recognizing the normal area inaccurately as abnormal is known as False Positive Rate (FPR)

$$FPR = \frac{FP}{FP + TN} \tag{18}$$

False Negative Rate (FNR):

FNR is the method of recognizing the anomalous area inaccurately as normal is known as False Negative Rate

$$FNR = 1 - \left(\frac{TP}{TP + FP} \right) \tag{19}$$

5.2 Comparative analysis:

5.2.1Tumor segmentation

The performance of our intended watershed segmentation approach is evaluated with that of the conventional K- means and FCM approaches based on accuracy, sensitivity, FPR, FNR and specificity and the table for the evaluation outcomes is illustrated below.

Table 1: Performance comparision of Proposed watershed segmentation techniques with the existing FCM and K-means techniques on account of (i) Accuracy (ii) Sensitivity (iii) Specificity (iv)FPR (v)FNR metrics

Measures	K-MEANS	FCM	**Proposed Watershed algorithm**
Accuracy	0.75096	0.844761	**0.96103**
Sensitivity	0.77088	0.858842	**0.967579**
Specificity	0.498934	0.65461	**0.866364**
FPR	0.22912	0.141158	**0.032421**
FNR	0.501066	0.34539	**0.133636**

Discussion:

Table 1 illustrates the performance of the proposed watershed segmentation with the other conventional techniques like K- means and FCM approaches based on accuracy, sensitivity and specificity. While viewing the comparison table, accuracy, sensitivity, specificity, FPR and FNR of our intended approach is 0.96103, 0.967579, 0.8663640, 0.032421 and 0.133636 correspondingly. It is possibly more when relating with that of the conventional K- means and FCM approaches. Therefore our intended watershed tumor segmentation approach yields improved segmentation outcome than the conventional approaches. The comparison graph for the tumor segmentation is illustrated in fig 6.

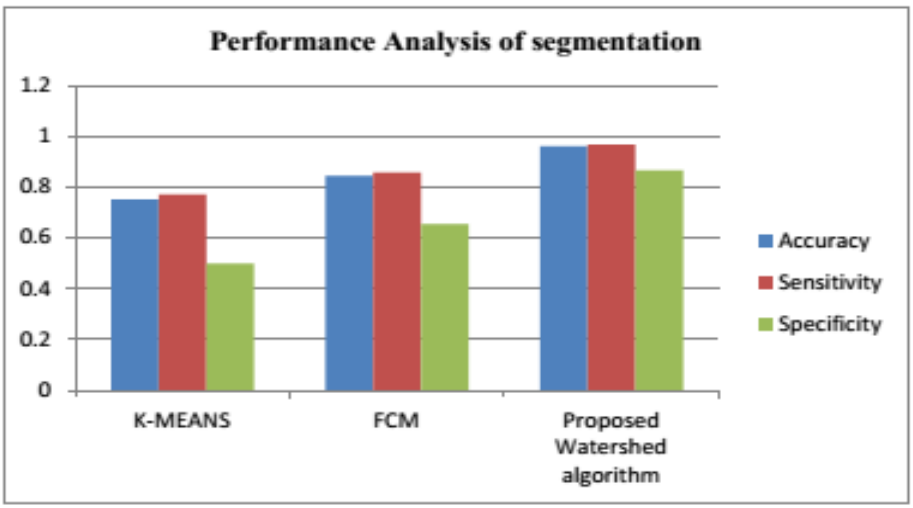

Fig 6: Performance graph analysis of the intended watershed segmentation approach with that of the conventional FCM and K-means approaches in terms of Accuracy, Sensitivity, Specificity

5.2.2 Normal and abnormal classification

The performance of our intended probabilistic neural network classifier (PNN) is examined by means of six statistical metrics namely, Accuracy, Precision, FDR, FAR, FRR and MCC. Then the classification outcome is related with that of the conventional NN and ANFIS approach.

False Discovery Rate (FDR)

It is the predicted proportion of discoveries and is computed by means of the following formula,

$$FDR = \frac{FP}{(TP + FP)} \tag{20}$$

False Acceptance Rate(FAR)

It is the ratio of the No of false acceptances to the No of attempts.

FAR= False Positive (21)

False Rejection Rate(FRR)

It is the ratio of the No of false rejection to the No of attempts.

FAR= False Negative (22)

Mathews correlation coefficient(MCC)

It is in essence a correlation coefficient amid the pragmatic and predicted binary categorization

$$\mathbf{MCC=} \frac{TP * TN - FP * FN}{\sqrt{(TP + FP)(TP + FN)(TN + FP)(TN + FN)}}$$

Table 2: Performance evaluation of the Proposed PNN classifier technique with the conventional classifier techniques in terms of (i) Accuracy (ii)Precision (iii)FAR (iv)FDR (v)FRR (vi)MCC metrics

Measures	ANFIS	Neural Network	Proposed PNN
Accuracy	0.8286	0.8571	**0.9857**
Precision	0.2	0.6667	**1**
FAR	12	10	**0**
FDR	0.8	0.6667	**0**
FRR	0	0	**1**
MCC	0.4052	0.5311	**0.9594**

Discussion:
Table 2 illustrates the performance of the intended probabilistic neural network classifier with the conventional NN and ANFIS approaches. Here the performance of the proposed probabilistic neural network is assessed by means of statistical metrics such as precision, accuracy, FDR,FAR,FRR and MCC values which is then related with that of the conventional neural network (NN) and ANFIS approach. In accordance with the comparative psychiatry in table (2) it is observed that our intended approach yields high performance ratio when related with the conventional approach. Therefore our intended probabilistic neural network (PNN) classifier categorizes the images more precisely than the conventional techniques.

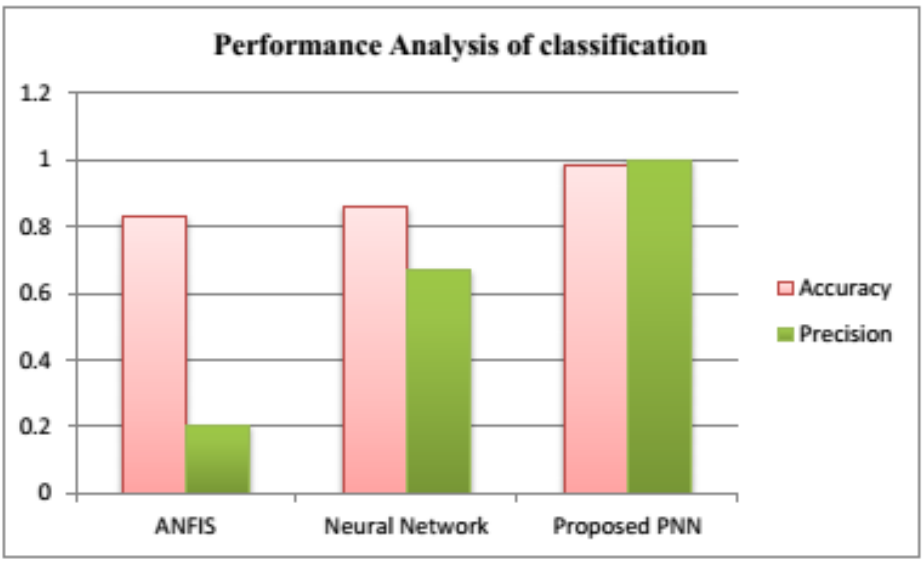

Fig 7: Performance graph psychiatry for the intended PNN classifier technique with the conventional classifier techniques in terms of (i) Accuracy (ii) Precision

5.2.3 Depth Quality Evaluation

The depth quality of an MRI images are obtained by means of the guided filter based depth computation. Table 3 illustrates that our intended guided filter based depth computation yields superior outcome as when related with that of the median filter based depth computation.

Table 3: Depth map assessment for the sample images from the database

Depth Rate		
images	**Median depth**	**Guided depth**
1	32.31454334	33.41529642
2	69.54678965	71.23183391
3	65.27058447	66.61731063
4	60.43267983	61.74607509
5	63.56723569	64.70230108
6	67.46789098	68.20130198
7	95.59251392	97.29614721
8	31.56577006	33.41529642

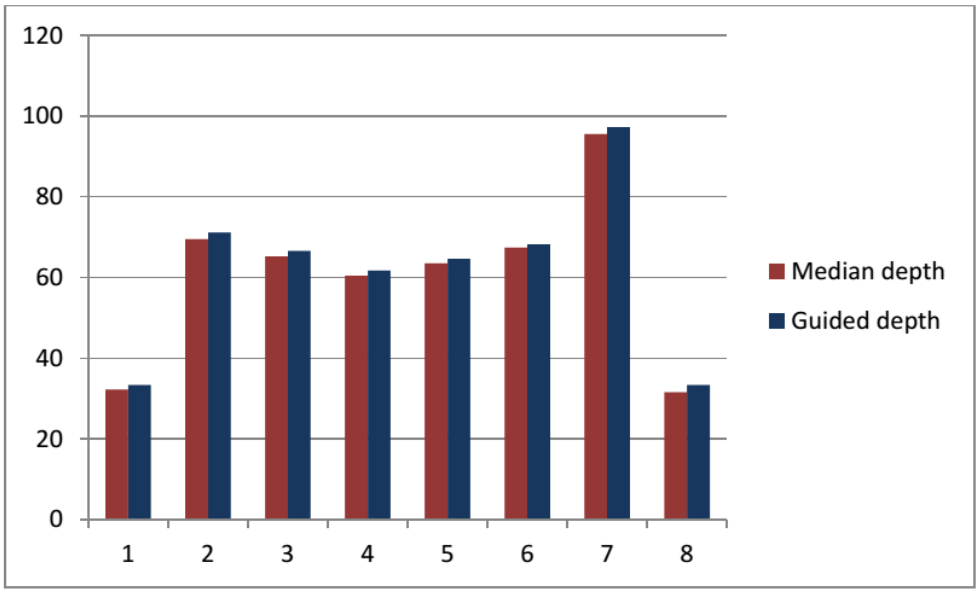

Fig 8: Depth Rate Graph

Fig 8 exhibits that our intended guided filter based depth quality is high than that of the median based depth quality

.

6 CONCLUSION

In our intended technique we completed two phases namely, i) classification, and ii) reconstruction. In the initial phase the Probabilistic neural network (PNN) classifier is employed for extorting the attributes. The comparative psychiatry of our intended

technique is related with that of the several conventional techniques such as ANFIS and NN. The comparison outcome reveals that our intended PNN classifier approach yields better accuracy, sensitivity and specificity values than the conventional approaches. In the next phase of 3D reconstruction, the skull stripped is reconstructed depending upon the assessment of depth map by means of guided filter. By means of the depth map, left view and right view images are produced and lastly the stereoscopic images were engendered to afford a sense of depth to the viewers by means of anaglyph glasses. Moreover, the separation and loss relics of the synthesized outcomes are successfully prohibited with less computation intricacy.

REFERENCES

[1] Naveenkumar, R., and S. Sanjay, "Morphological Image Processing Approach for 2D to 3D Reconstruction of MRI Brain Tumor from MRI Images." The International Journal of Science and Techno ledge, Vol.2, No. 5, 2014.

[2] Guo, Fan, Jin Tang, and HuiPeng, "Automatic 2D-to-3D Image Conversion based on Depth Map Estimation", International Journal of Signal Processing, Image Processing and Pattern Recognition, Vol.8, No.4, pp.99-112, 2015.

[3] Sindhushree. K. S, Mrs. Manjula. T. R, K. Ramesha, "Detection And 3d Reconstruction Of Brain Tumor From Brain MRI Images", International Journal of Engineering Research & Technology, Vol.2, No.9, 2013.

[4] Konrad, Janusz, Meng Wang, PrakashIshwar, Chen Wu, and Debargha Mukherjee. "Learning-based, automatic 2d-to-3d image and video conversion", IEEE Transactions on Image Processing, Vol.22, No.9, pp.3485-3496, 2013.

[5] Kim, HakGu, and ByungCheol Song, "Automatic object-based 2D-to-3D conversion", In IVMSP Workshop, 2013 IEEE 11th, pp. 1-4, 2013.

[6] Kavita A. Ugale, Dr. S.T. Patil, "International Journal of Advanced Research in Computer Science and Software Engineering", Vol.5, No.7, 2015.

[7] Lee Sang-Hyun, Park Dae-Won, Jeong Je-Pyong and Moon Kyung-Il, "Conversion 2D Image to 3D Based on Squeeze function and Gradient Map", Vol.8, No.2, pp.27-40, 2014.

[8] S.Vimala, BobiNath, "A Survey on Medical Images", International Journal of Advanced Research in Computer Science and Software Engineering, Vol.5, No.10, 2015.

[9] Arakeri, Megha P., and G. Ram Mohana Reddy, "An effective and efficient approach to 3D reconstruction and quantification of brain tumor on magnetic resonance images", International Journal of Signal Processing, Image Processing and Pattern Recognition, Vol.6, No.3, 2013.

[10] Roslan, Rosniza, NursuriatiJamil, and Rozi Mahmud, "Skull stripping magnetic resonance images brain images: region growing versus mathematical

morphology", International Journal of Computer Information Systems and Industrial Management Applications, No.3, pp.150-158, 2011.

[11] Somasundaram, K., and P. Kalavathi, "Brain segmentation in magnetic resonance human head scans using multi-seeded region growing", The Imaging Science Journal,Vol.62, No.5 pp.273-284, 2014.

[12] Lopes, Sayali, and Deepak Jayaswal, "A Methodical Approach for Detection and 3-D Reconstruction of Brain Tumor in MRI", International Journal of Computer Applications, Vol.118, No.17, 2015.

[13] Borse, Megha, S. B. Patil, and B. S. Patil, "Literature Survey For 3d Reconstruction of Brain MRI Images", International Journal of Research in Engineering and Technology, Vol.2, No.11 2013.

[14] Chitradevi, D., and M. Krishnamurthy. "A Survey on MRI based automated Brain Tumor Segmentation Techniques." International Journal,Vol.3, No.11, 2014.

[15] Omar, Salima, AsriNgadi, and Hamid H. Jebur. "Machine learning techniques for anomaly detection: an overview", International Journal of Computer Applications, Vol.79, No.2, 2013.

[16] Shreepad S. Sawant, Preeti S. Topannavar, "Introduction to Probabilistic Neural Network –Used For Image Classifications", Vol.5, No.5, 2015.

[17] Gondal, A. H., & Khan, A review of fully automated techniques for brain tumor detection from MR images, International Journal of Modern Education and Computer Science, Vol.5, No.2, 2013.

[18] Karthik, Menaka, and, Chellamuthu, "A comprehensive framework for classification of brain tumour images using SVM and curvelet transform", International Journal of Biomedical Engineering and Technology,Vol.17, No. 2, pp.168-177, 2015.

[19] Arakeri, Megha P., and G. Ram Mohana Reddy, "Computer-aided diagnosis system for tissue characterization of brain tumor on magnetic resonance images", Signal, Image and Video Processing,Vol.9, No. 2, pp.409-425, 2014.

[20] S. U. Aswathy, G. G. Deva Dhas and S. S. Kumar, "A survey on detection of brain tumor from MRI brain images," Control, Instrumentation, Communication and Computational Technologies (ICCICCT), 2014 International Conference on, Kanyakumari, pp. 871-877, 2014.

[21] Y. Han, "2D-to-3D Visual Human Motion Converting System for Home Optical Motion Capture Tool and 3-D Smart TV," in IEEE Systems Journal, Vol. 9, No. 1, pp. 131-140, 2015.

[22] Yang, Na-Eun, Ji Won Lee, and Rae-Hong Park. "Depth map generation using local depth hypothesis for 2D-To-3D conversion." International Journal of Computer Graphics & Animation Vol.3, No. 1, 2013.

[23] Jung, Cheolkon, Lei Wang, Xiaohua Zhu, and Licheng Jiao, "2D to 3D conversion with motion-type adaptive depth estimation", Multimedia Systems, Vol.21, No.5, pp.451-464, 2015..

[24] W. Huang, X. Cao, K. Lu, Q. Dai and A. C. Bovik, "Toward Naturalistic 2D-to-3D Conversion," in IEEE Transactions on Image Processing, vol. 24, no. 2, pp. 724-733, Feb. 2015.

[25] Liu, Wei, Yihong Wu, Fusheng Guo, and Zhanyi Hu. "An efficient approach for 2D to 3D video conversion based on structure from motion", The Visual Computer, Vol.31, No.1, pp.55-68, 2015.

[26] Jung, Cheolkon, Lei Wang, Xiaohua Zhu, and Licheng Jiao, "2D to 3D conversion with motion-type adaptive depth estimation", Multimedia Systems,Vol.21, No.5, pp.451-464, 2015.